

Nanochannel Materials for Artificial Photosynthesis

Gion Calzaferri ¹⁾ and André Devaux ²⁾

¹⁾ Department of Chemistry and Biochemistry University of Bern, Freiestrasse 3, CH-3012 Bern, Switzerland.

²⁾ Physikalisches Institut, Westfälische Wilhelms-Universität, D-48149, Münster, Germany

Abstract

We present a short historical account on the developments in photochemical energy transformation and storage of solar energy. The focus is on artificial photonic antenna systems and photocatalytically active layers that have been built by incorporating organic dyes, complexes, metal cations and clusters into one-dimensional nanochannel materials. We show that zeolite L (ZL) as a host material allows for the design and preparation of a large variety of highly organized host-guest systems. The combination of tuneable host morphology with the possibility of obtaining highly organized molecular patterns of guests leads to a variety of potential optical and photoelectronic applications. Strongly absorbing systems exhibiting efficient FRET along the *c*-axis of the ZL crystals are accessible by sequential inclusion of multiple types of dyes. These new light-harvesting materials offer unique possibilities as building blocks for solar-energy conversion devices. A novel generation of luminescent concentrators is based on such hybrid materials. A complementary approach consists in integrating photochemically active substances into ZL monolayers coated on an electrode and taking advantage of intrazeolite processes for designing a reversible electrode for photocatalytic water oxidation. The photoelectrochemical water splitting capability of systems based on Ag⁺/AgCl/Ag_n-ZL photoanodes is discussed.

1 Introduction

Sunlight is the fundamental energy source sustaining life on earth. The production of food, oxygen, and fossil fuels depend on the conversion of solar into chemical energy by biological photosynthesis. This process converts sunlight, water and carbon dioxide, which are abundant raw materials, into reduced organic species and oxygen.¹ The processed materials serve in turn as food or fuel for all life forms. Many different organisms, from algae and bacteria to green plants, are known to perform photosynthesis. The net primary production (NPP) of organic carbon through photosynthesis has been estimated to be in the order of 105 Pg (1 Pg = 10¹⁵ g) per year, with roughly equal contributions from land and oceans.² Thus, the photosynthetic process constitutes an important CO₂ sink.

The sun provides our earth with about 178'000 TW, as shown in the energy balance scheme in Figure 1. This amount corresponds roughly to 14'000 times our current "technical power consumption". The effects of incoming sunlight can be divided into three categories: about 30% of it is directly reflected back to space; while 46% is absorbed by the earth, where it is converted into heat and reradiated. The water cycle, winds and photosynthesis are generated by the remaining 24% of the solar energy. Geothermal heat that can be tapped from earth's core makes up for about 30 TW, while the gravitational pull of the moon generates roughly 3 TW as tidal power. Only about 0.056% of the solar radiation hitting the earth is used for the life sustaining photosynthesis.³

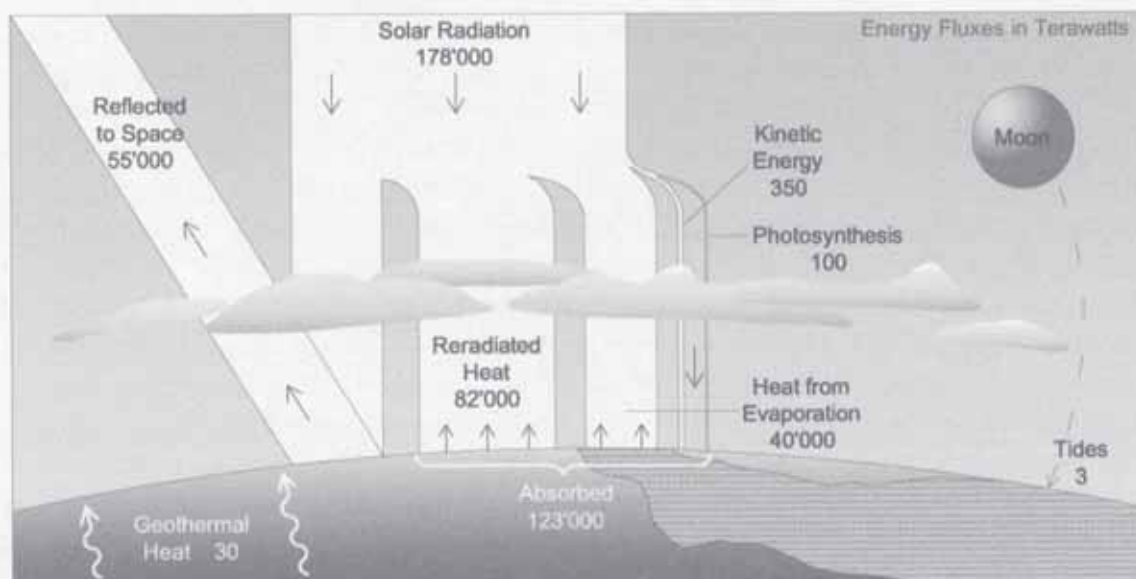


Figure 1 Energy balance of the earth. Roughly 178'000 TW (1 TW = 10^{12} W) of solar energy strike the earth. This corresponds to about 14'000 times our actual "technical power consumption". About 30% of this energy flux is reflected into space, while 46% is absorbed by the earth and converted into reradiated heat. The remaining 24% are used to power the water cycle, generate winds and drive photosynthesis. Only 0.056% of the total energy flux drives the photosynthesis of green plants, which is the basis of all current life on Earth

First ideas for using this ample renewable energy supply arose in the late 19th to early 20th centuries. Wilhelm Ostwald, who is often considered as being the father of physical chemistry, argued in 1911 that humanity should cover its energy needs primarily by means of solar energy.⁴ Inspired by the ability of green plants to convert solar into chemical energy, Giacomo Ciamician predicted in 1912 that the future of fuels would lie in the production of chemical fuels by means of photosynthesis.⁵ In the 1950s, researchers from the US company Bell discovered that silicon rectifiers exhibited a stronger current when exposed to sunlight. As a consequence, Bell developed in 1954 the first silicon solar cells (with a device efficiency of 4% to 6%). The first tests of solar cells in space took place in 1958

with the launch of the Vanguard I satellite. However, the first serious attempts to promote technical use of solar energy on a large scale came as a consequence of the first oil crisis from 1973 to 1974. In October 1973, a new war broke out between Israel and its Arabic neighbors. As the Arabic states could not secure a military victory, several oil exporting countries decided to turn to "economic warfare". On October 16th, all oil exports were stopped with immediate effect. In the aftermath of these events, a greater interest was given to projects aiming at the reduction of our dependency on crude oil. Nowadays transformation of solar energy has become a respectable business with an annual growth rate of about 40%. The rapid engineering and technological advances of the last few years have extended the subject of solar energy conversion from science into politics and economics.

In this article, we will be discussing structurally organized and functionally integrated artificial systems that are capable of elaborating the energy and information input of photons to perform specific functions. Elaborating materials capable of performing functions such as processing and information storage, sensing microscopic environment on a nanoscale level or transforming and storing solar energy, is a fascinating topic of modern photochemistry.^{6,7} One-dimensional channel materials, such as zeolites and mesoporous silicas, are very attractive hosts for the preparation and investigation of hierarchically organized structures, presenting a successive ordering from the molecular up to macroscopic scale.⁷⁻¹⁰

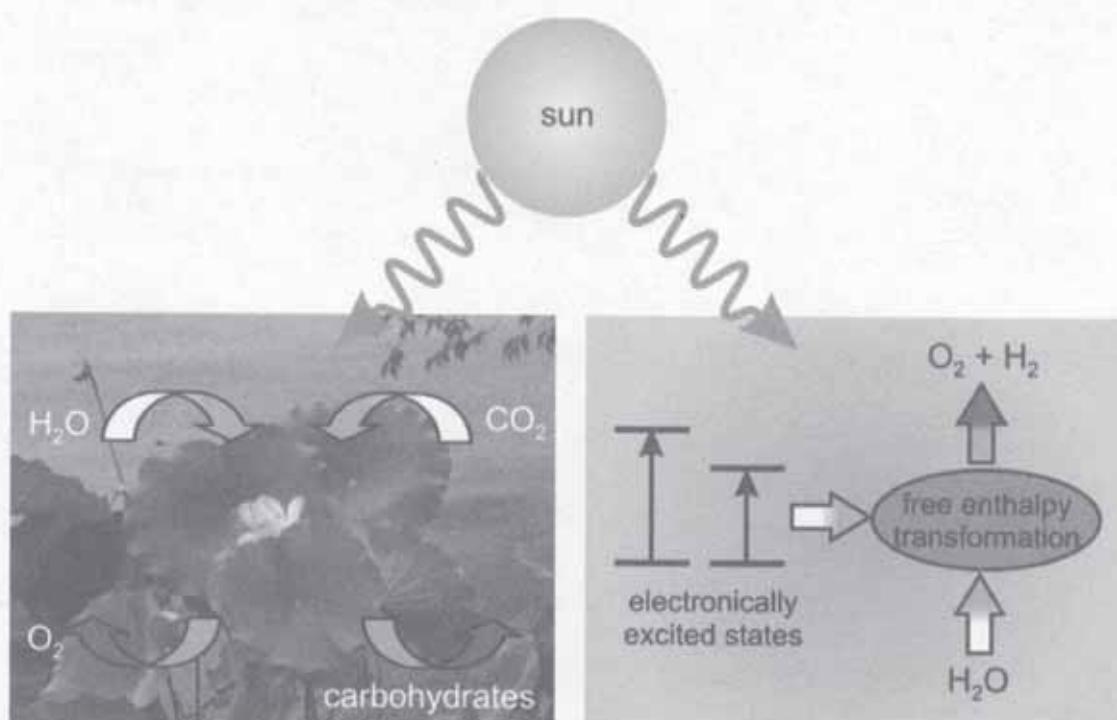


Figure 2 Quantum solar energy conversion and storage. Left: Illustration of the principle and the beauty of natural photosynthesis. Right: Principle of an artificial quantum solar energy conversion and storage system

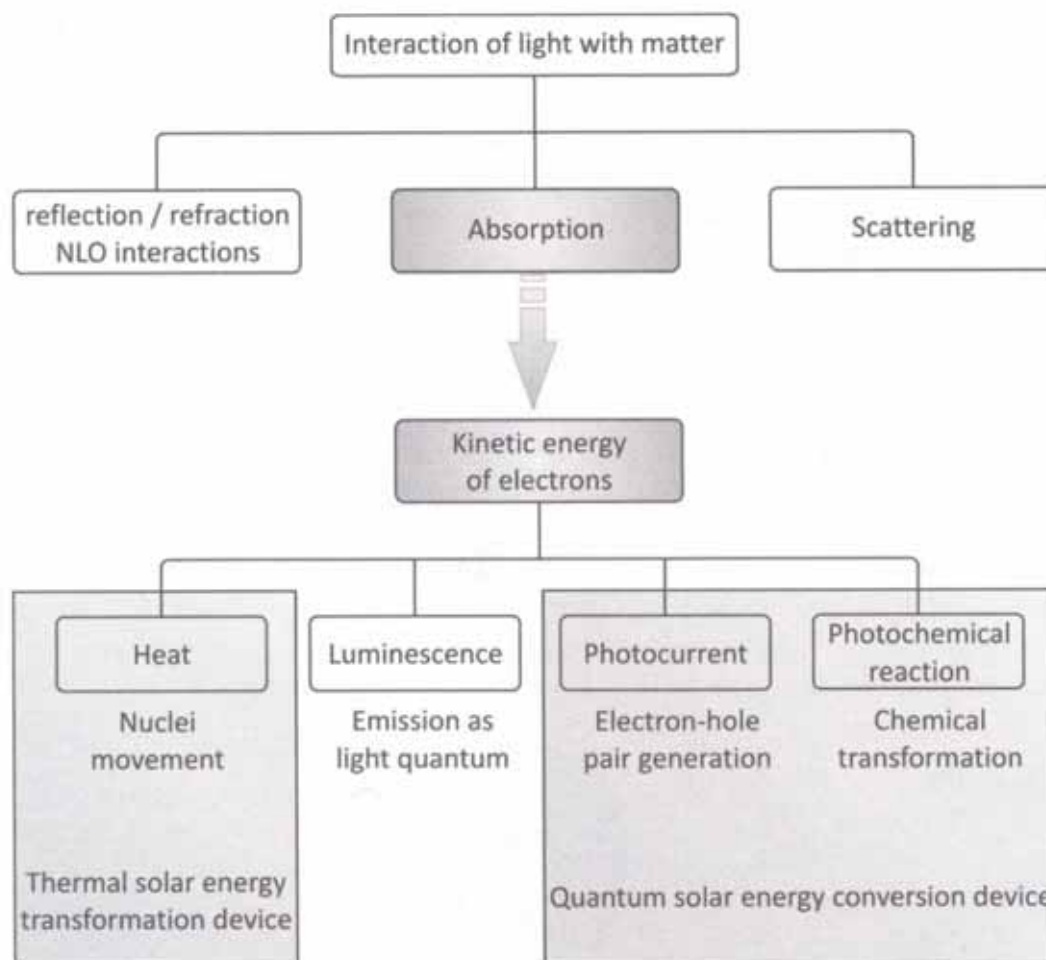


Figure 3 Interaction of light with matter and transformation of solar energy

Natural photosynthesis – as illustrated on the left hand side of Figure 2 – is an essential process for life on Earth, but the overall thermodynamic efficiency for the production of fuel is low and depends very much on optimal soil, temperature and humidity conditions. The natural process has many other important tasks to fulfill than just conversion of solar light into a chemical fuel. A long-standing challenge has therefore been the development of a practical artificial photosynthetic system that is able to carry out the energy conversion process not by duplicating the self-organization and reproduction of the biological system nor the aesthetic beauty of plants and trees, but rather by being able to use sunlight to drive a reaction of abundant materials to produce a fuel (right hand part of Figure 2).^{6,7,11-14}

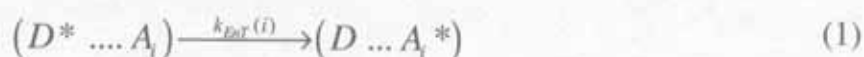
The present article will be focused on artificial photonic antenna systems and photocatalytically active layers. The systems being discussed have been built up by incorporating organic dyes, metal complexes, cations or clusters into materials with one-dimensional nanochannels. Before going into more details, it is useful to recall a

simplified – but yet useful – overview of the possible light-matter interactions, as sketched in Figure 3. Light that has been absorbed by matter is first stored for a very short time as kinetic energy of electrons. This energy can either be transformed into kinetic energy of the nuclei and released as heat or be emitted as light of somewhat longer wavelength. It can also create an electron-hole pair which can e.g. be used to drive a photocurrent. A fourth possibility to use this energy is as a reagent for matter alteration in a photochemical reaction. Thermal solar energy conversion has many important applications which will, however, not be addressed in this article. Quantum solar energy conversion means direct utilization of the electronic excitation energy by creating photovoltage and photocurrent or by transforming the electronic excitation energy through a photochemical or photocatalytic reaction into free enthalpy stored as a chemical fuel.^{6,7,11-15}

2 Artificial Antenna Systems

Green plants have developed very sophisticated tools for trapping light and transporting electronic excitation energy in their antenna system. We understand the detailed structure of the purple bacteria's antenna system. It consists of regular arrangements of chlorophyll molecules held at fixed positions by means of proteins.^{6,15} Light absorbed by any of these chromophores is transported to the reaction centre, providing the energy necessary for chemical processes to be initiated. A green leaf consists of millions of such well organized antenna devices.

The understanding of the basic principles that govern the transport of electronic excitation energy is very advanced and goes back to the pioneering work of Theodor Förster.¹⁶ A chlorophyll molecule consists essentially of a positively charged backbone with some delocalized electrons. The energy of an absorbed photon is transformed into kinetic energy of one of these delocalized electrons. This fast moving electron causes an oscillating electromagnetic field that can interact with a neighboring acceptor molecule A , if the latter bears states that are in resonance with the excited state of the donor D^* . Thus the excitation energy can be transferred from one molecule to another. The radiationless electronic excitation energy transfer (EnT) is due to the very weak near field interaction between excited configurations of the initial state ($D^* \dots A_i$) and of the final state ($D \dots A_i^*$). The Förster resonance energy transfer (FRET) mechanism involves no orbital overlap between the donor and acceptor molecules, and thus no electron transfer occurs.



In such a system the "optical electrons" associated with individual chromophoric units preserve essentially their individual characteristic. The donor D and the acceptor A can be the same kind of molecules or be different. Förster observed that the rate constant k_{EnT} for the transfer from one electronic configuration to the other can be expressed as a product of three terms:

$$k_{EnT} \propto G \cdot DA \cdot S \quad (2)$$

The geometrical term G describes the dependence of the rate constant on the distance and angle between the electronic transition dipole moments (ETDM) of the donor and the acceptor. DA specifies the chromophores involved, by taking into account the resonance condition as well as the photophysical properties of the donor, while the factor S takes into account the environment.

Our design of a model mimicking the key functionality of the green plants antenna system was inspired by the experience we had with different zeolite materials.¹⁷⁻¹⁸ The properties of molecules, complexes and clusters inside cavities and channels of zeolites – apart from the field of catalysis – have been investigated for many years.¹⁹⁻³⁰ A one-dimensional channel system has the advantage of being the simplest possible choice, as is illustrated in Figure 4. The donor molecules are represented in light grey and the acceptors in dark grey. The donor, being excited by photon absorption, transfers its electronic excitation to an unexcited neighbor. After series of such steps, the electronic excitation reaches a luminescent trap (acceptor molecule) and is then released as luminescence. The acceptors are thought to mimic the "entrance to the reaction centre" of the natural antenna. The dimensions given in Figure 4 correspond to the pore opening and centre to centre distance between two neighboring channels in zeolite L (ZL). According to Förster theory, the largest EnT rate constant is observed if the ETDM are oriented parallel to the channel axis. Electronic excitation energy transport can be extremely fast in such systems because of the low dimensionality.

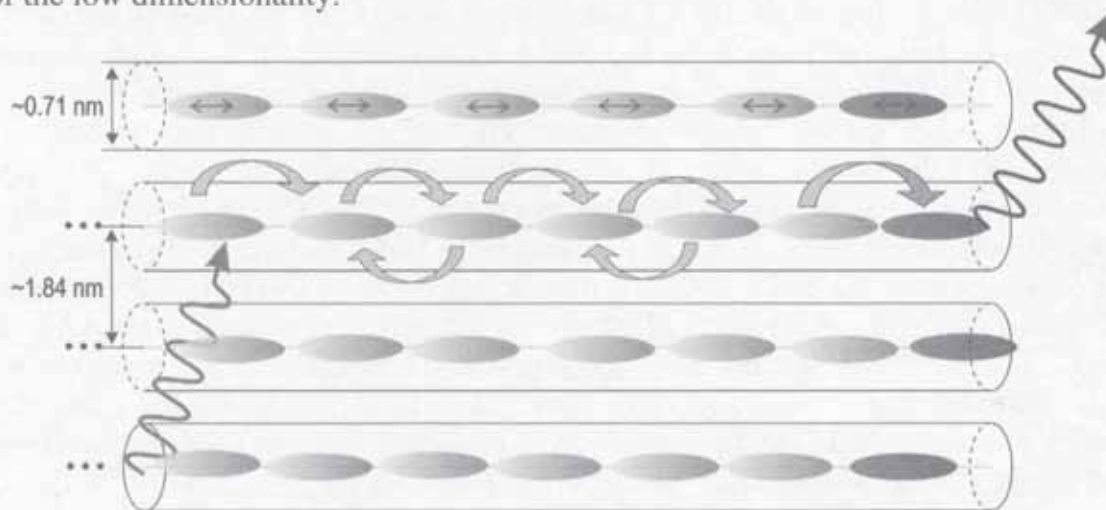


Figure 4 Schematic overview of an artificial photonic antenna. The chromophores are embedded in the channels of the host. The light grey dyes act as donor molecules that absorb incoming light and transport the electronic excitation energy via FRET to the dark grey acceptors shown at the channel ends on the right. The process can be analyzed by measuring the emission of the acceptors and comparing it with that of the donors. The double arrows indicate the orientation of the ETDM

Different materials bearing one-dimensional channels can be envisaged for realizing the situation sketched in Figure 4. We found that ZL is an excellent host for the supramolecular organization of organic dyes. The synthesis of ZL crystals of different morphologies in the size range of 30 nm up to about 10'000 nm is well established.³⁰⁻³⁹ We therefore focus on systems based on ZL as a host. The reasoning is, however, also valid for other host materials with similar properties. The structure and morphology of ZL is illustrated in Figure 5. The primary building unit of the framework consists of TO₄ tetrahedrons where T represents either Al or Si. The channel system exhibits hexagonal symmetry. The molar composition of ZL is (M⁺)₉[(AlO₂)₉(SiO₂)₂₇]·nH₂O, where M⁺ are monovalent cations, compensating the negative charge resulting from the (AlO₂)-unit. *n* is equal to 21 in fully hydrated materials, and 16 for crystals equilibrated at 22 % relative humidity.³⁸⁻⁴⁰ It is useful to imagine ZL as consisting of a bunch of strictly parallel channels as shown in Figures 4 and 5(A). The channels have a smallest free diameter of about 0.71 nm, and the largest diameter inside is 1.26 nm. The distance between the centres of two neighboring channels is 1.84 nm. Each ZL crystal consists of a large number of channels (*n_{ch}*) which can be estimated as follows:⁷

$$n_{ch} = 0.267(d_z)^2 \quad (3)$$

where *d_z* is the diameter of the crystal in nm. For example, a crystal with a diameter of 600 nm features nearly 100'000 strictly parallel channels. The ratio of void space available in the channels with respect to the total volume of a crystal is about 26%. An important consequence is that ZL allows, through geometrical constraints, the realization of extremely high concentrations of well oriented molecules that behave essentially as monomers. A 30 nm by 30 nm crystal can accept up to nearly 5'000 dye molecules that occupy 2 unit cells; while a 60 nm by 60 nm crystal can host nearly 40'000. Many different molecules, complexes and clusters have been inserted into the channels of ZL.

We already stated that the focus is on situations where molecules behave in the states of interest as individuals, which means that the "optical electrons" associated with the chromophoric units preserve essentially their individual characteristics. They can, however, communicate with each other. We are interested in molecules that are so large that they can neither pass each other inside of the channels nor sit on top of each other, as illustrated in Figure 6. The geometrical constraints imposed by the host determine the orientation of the dye molecules inside the channels and hence the orientation of the ETDM. Exciton splitting becomes important at sufficiently short distances between the ETDM of neighboring chromophores.^{7,41-44}

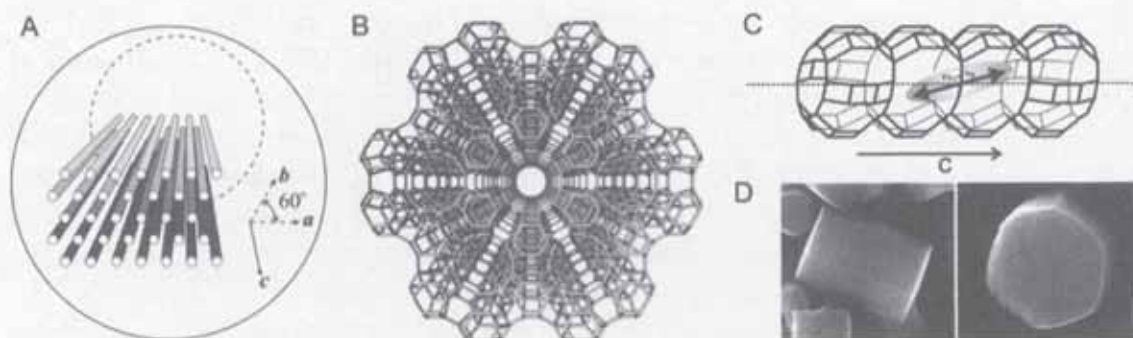


Figure 5 Zeolite L. (A): Schematic view of the channels. (B): Top view of the framework of ZL, illustrating the hexagonal structure. It shows a channel surrounded by six neighboring channels. The centre to centre distance between two channels is 1.84 nm. (C): Side view of a channel that consist of 0.75 nm long unit cells with a Van der Waals opening of 0.71 nm at the smallest and 1.26 nm at the widest place. The double arrow indicates the ETDM of an inserted molecule. (D): SEM image of ZL crystals with a diameter of about 600 nm

From the whole volume of the zeolite only a part, namely the channels, is available for the guest species. It is therefore convenient to introduce a parameter bearing the information on dye concentration that is based on purely geometrical (space-filling) properties of the host, i.e. showing to what extent the ZL channels are filled with dye molecules. The loading, or occupation probability, p of a dye-ZL material is defined in equation (4):

$$p = \frac{\text{number of occupied sites}}{\text{total amount of sites}} \quad (4)$$

The sites n_s represent the number of unit cells occupied by one dye molecule. It can, for example, be equal to 1, 2 or larger. n_s must not necessarily be an integer number. The loading ranges from 0 for an empty ZL to 1 for a fully loaded one. The dye concentration of a loaded ZL material $c(p)$ in units of mol/L can be expressed as a function of the loading as follows:

$$c(p) = 0.752 \frac{p}{n_s} \left(\frac{\text{mol}}{\text{L}} \right) \quad (5)$$

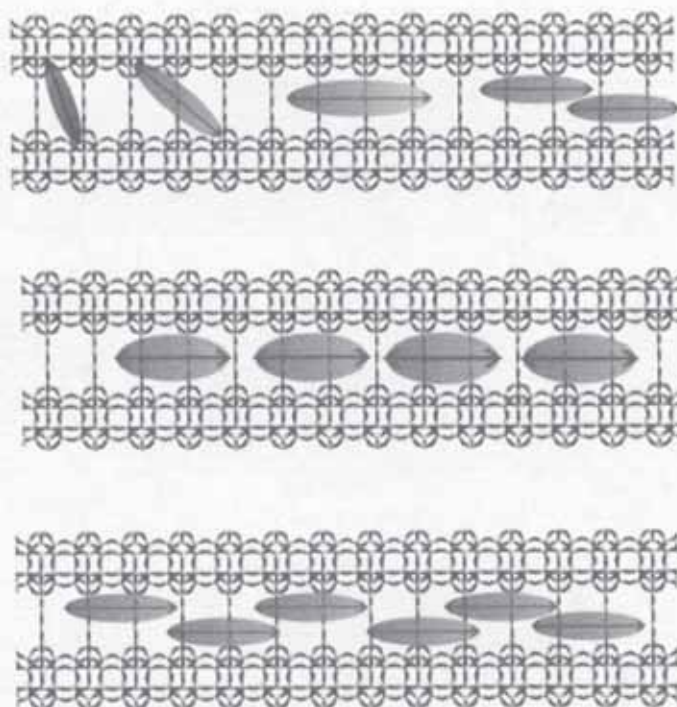


Figure 6 Packing of dyes in the channel, explained by means of a simplified view of different orientations and molecular arrangements in a channel. The orientation of the ETDM is indicated by a double-arrow. Top: the molecule on the left is small enough to fit into one unit cell and its shape is such that the ETDM is oriented nearly perpendicular to the channel axis. Its neighbor is slightly larger and thus occupies two unit cells and is oriented at an angle of about 45° . The next molecule is so large that it can only align parallel to the channel. On the right we illustrate a situation where two molecules come so close that their orientation and their optical properties are influenced by the packing. Middle: orientation of large molecules which align parallel to the channel axis because of their size and their shape. Bottom: Stacking of molecules of appropriate size and shape, leading to excitonic states

Försters theory leads to a simple expression for the EnT rate constant that contains only experimentally accessible parameters.¹⁶ This is of great value. The same is true for Davydows theory to describe exciton coupling in such systems.⁴³ Both have been found to be very useful for designing and understanding organized systems based on nanochannel materials.^{7,9,18} The FRET process can be extended from the inside of a crystal to its environment (or vice versa) by means of so called stopcock molecules.⁴⁵⁻⁴⁶ Such stopcock molecules consist of a head group that is too large to pass the pore opening and a tail that fits into the channel. These chromophores are therefore located at the zeolites basal surfaces and can promote communication between dyes inside the crystal and the outside world.

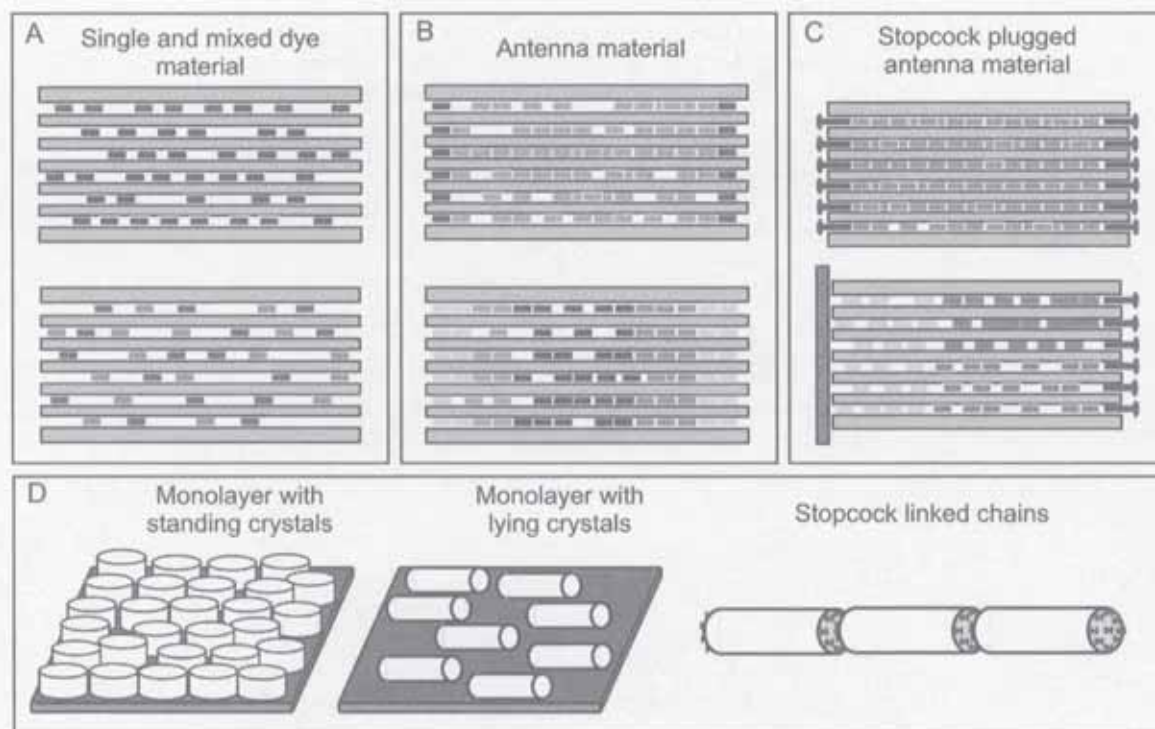


Figure 7 Schematic representations of supramolecularly organized dye-ZL composites. (A): Single and mixed dye materials are obtained by either loading ZL crystals with one kind of dye (top) or by simultaneous insertion of different dye molecules (bottom). (B): Antenna materials, prepared by sequential insertion of different dyes. (C): Stopcock-plugged antenna material, obtained by modifying either bidirectional (top) or mono directional (bottom) antenna materials with specific closure molecules, called stopcocks. (D): Organization of ZL crystals. Oriented monolayers of either standing or lying ZL crystals on a substrate and chains of crystals linked by the interaction between stopcocks located at the channel entrances

It has been shown that ZL as a host material allows for the design and preparation of a large variety of highly organized host-guest systems. Relevant types are illustrated in Figure 7. Important steps in the development of these composite materials were the sequential filling with different dyes, the invention of the stopcock principle, the discovery of quasi 1-D energy transfer, the preparation of unidirectional energy transfer material and finding ways to create hybrid materials fully transparent in the visible range. The latter is important for spectroscopic investigations, since ZL crystals exhibit considerable light scattering due to their size and refractive index. For a more detailed discussion of this we refer to refs. ⁷ and ⁴². ZL is the only currently available microporous material allowing the realization of the full range of organizational patterns presented here. It is, however, interesting and worthwhile to investigate to what extent other zeolite based materials but also materials based on mesoporous hosts can be used for extending these organizational patterns.^{9,47}

The range of possibilities for filling one-dimensional channels with different suitable guests has been shown to be much larger than one might expect at first glance.^{7,9,42} Geometrical constraints imposed by the host structure lead to supramolecular organization of the guests in the channels. The supramolecular organization of dyes inside the ZL channels is what we call the first stage of organization. It allows light harvesting within the volume of a dye-loaded ZL crystal and also radiationless transport of energy to either the channel ends or centre. One-dimensional FRET transport can be realized in these guest-host materials as illustrated in Figure 8.

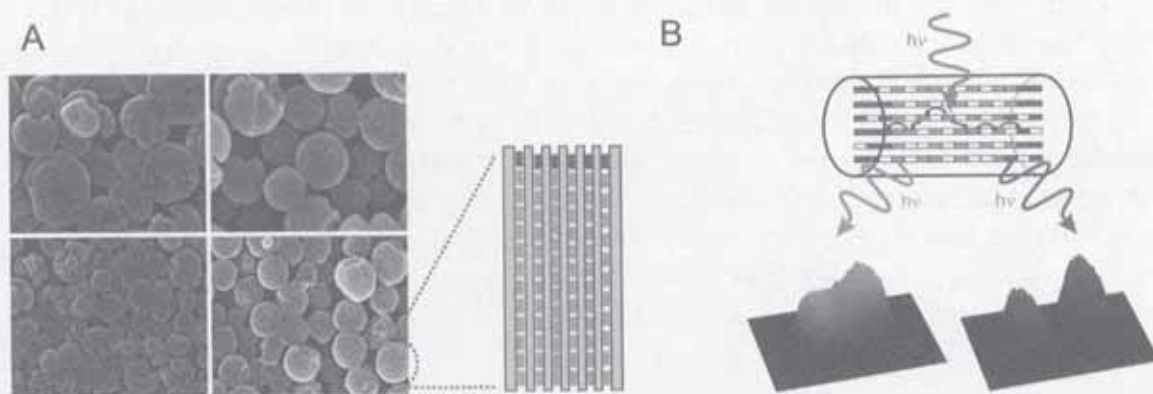


Figure 8 Dye-ZL antenna systems. (A): SEM images of disc-shaped ZL crystals oriented as compact monolayers on a substrate. The inset shows an unidirectional two-dye antenna material. The ZL channels are first filled with a donor molecule (light grey squares) and subsequently with a thin layer of acceptors (dark grey squares). (B): Scheme explaining the working principle of a bidirectional two-dye antenna material. A donor molecule, after being excited by photon absorption, can transfer its excitation energy to neighbouring molecules in a radiationless process. Once the excitation energy reaches the acceptor layer, it is trapped in space and released either as luminescence or converted into heat

The second stage of organization is realized by coupling either an external acceptor or donor stopcock fluorophore at the ends of the ZL channels, which can then trap or inject electronic excitation energy. The third stage of organization is obtained by interfacing the material to an external device via a stopcock intermediate; see Figure 9. A possibility to achieve higher levels of organization is by controlled assembly of ZL crystals into oriented structures and preparation of monodirectional materials.^{7,9,45-52} The usually strong light scattering of ZL can be suppressed by refractive index matching and avoidance of microphase separation in hybrid polymer/dye-ZL materials.⁵³

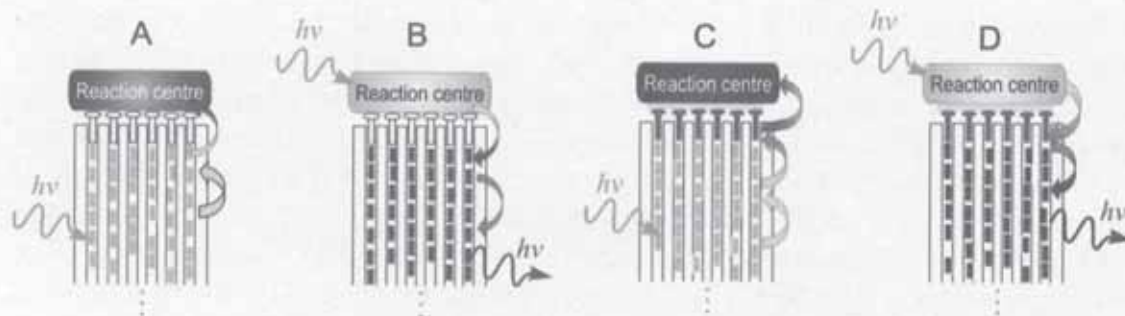


Figure 9 Communication of guests with an external reaction centre via FRET. Non fluorescent stopcock molecules can be used if they act as insulating or protecting chemical linkers between the dyes inside the channels and the chromophores located in the reaction centre. We illustrate in (C) and (D) that a thin insulating part between the luminescent stopcock and the reaction centre is usually desirable if the stopcocks are luminescent molecules in order to avoid direct contact which might lead to electron transfer or other undesirable reactions. The insulating part can e.g. be covalently bound to either the stopcock or the reaction centre. The distance between donors and acceptors should be shorter than the Förster radius if efficient FRET is desired

2.1 Applications

The combination of tuneable host morphology, with highly organized guest molecular patterns and the possibility to arrange nano- and micro-crystals leads to a large variety of potential optical and photoelectronic applications of dye-ZL materials. Strongly absorbing systems exhibiting efficient FRET along the c-axis of the crystals can be realized by inclusion of multiple dye types. These materials form a basis for novel light-harvesting devices. The FRET processes can be fine-tuned by appropriate choice of dyes, whereas the ordering of the molecules can be extended to the macroscopic level by clever arrangement of the hosts. The robust ZL framework can further be selectively functionalized at the external crystal surfaces and at the pore entrances.

These new materials offer unique possibilities as building blocks for solar-energy conversion devices. A novel type of dye-sensitized solar cell is sketched in Figure 10 (B-C). The devices consist of a light harvesting unit coupled to thin active layer, where charge separation occurs, via a thin insulating layer. The light harvesting unit – its working principle is illustrated in Figure 10 (A) – is build up by arranging dye-loaded crystals of 50 nm to 200 nm length into compact monolayers. The light is first absorbed over a broad spectral range in the ZL-antenna material. Since the ZL channels are oriented perpendicularly to the semiconductor surface, the excitation energy is transported towards the ZL-semiconductor interface by means of FRET. From there, FRET to the semiconductor takes place across a very thin insulating layer. The insulating layer is needed to avoid short-circuiting the device. The injected energy can now be used to drive the charge-separation process in the

active medium.⁵⁴ The dye-ZL building blocks can also be used to create luminescent solar concentrators (LSC), which can in turn be coupled to solar cells. The concept of LSCs has been known since about 50 years.⁵⁵⁻⁵⁸ A LSC is a transparent plate containing luminescent chromophores. Light enters the face of the plate, is absorbed and subsequently re-emitted. The emitted light is trapped by total internal reflection and guided to the edges of the plate, where it can be converted to electricity by a solar cell. As the edge area of the plate is much smaller than the face area, the LSC operates as a concentrator of light. A major loss is caused by self-absorption due to overlap between the dye's absorption and emission spectra. Previous efforts to solve this problem have not been successful so far. Recently, however, new materials and techniques have become available to solve the major problems, rekindling interest in LSCs.⁵⁹⁻⁶⁰ Our solution to solve the self-absorption issue is to use a well designed dye-ZL antenna material.⁶¹ Absorption and emission spectra are separated by employing an absorbing dye present in large amounts, and a monolayer of emitting dyes.

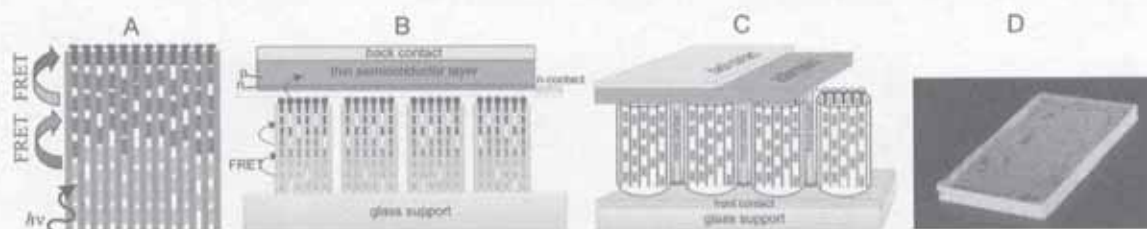


Figure 10 New building blocks for solar-energy-conversion devices. (A): working principle of the dye-ZL antenna material, consisting of nanochannels containing two types of dye molecules in the channels and one type of stopcock. Light absorbed by the molecules included in the channels travels to the stopcock heads radiationlessly, via FRET. (B and C): Principle of dye-sensitized solar cells.⁵⁴ Arranging crystals of 50 nm to 200 nm length with their channel axes perpendicular to the surface of a semiconductor allows transport of the excitation energy toward the ZL-semiconductor interface by FRET. The semiconductor layer can be very thin, because the electron-hole (n-p) pairs form near the surface. The transfer of electrons from the antenna to the semiconductor is prevented by introducing a thin insulating layer. Scheme (B) shows the operation principle of thin-layer silicon devices, while scheme (C) represents that of organic or plastic solar cells. The white area on top of the head is an insulating part directly integrated into the stopcock. The ZL material is enlarged with respect to the rest of the device. (D): Small dye-ZL based fluorescent concentrator (2 cm by 1 cm)⁶¹

Another issue with classical LCSs is photo bleaching of organic dye molecules embedded in the polymer matrix. The photostability of many dyes is considerably improved by embedding them into ZL. The geometrical constraints imposed by the channels can protect the guest species from photochemical decomposition processes, provided that the channels are well plugged by means of stopcock molecules so that leaching of the dyes and diffusion of small molecules from the outside into the

channels are blocked.^{7,9,61} The inorganic environment improves the photostability of inserted dyes by being less reactive than an organic matrix. The properties of dye loaded ZL materials outlined above make them very desirable for the development of optically active materials such as LCSs, lenses, nanostructured materials for optical data storage, or for improvement of a polymer's chemical-physical properties.⁶² For many applications, the host-guest systems have to be inserted into a polymer matrix while maintaining transparency in the visible range.⁶³ A drawback of ZL particles is their pronounced light scattering in the visible range. Based on dispersion and refractive index matching experiments with nanosized, dye-loaded ZL crystals, a procedure for preparing transparent polymer-ZL materials has been developed.⁵³ Photographic images of a series of such hybrid materials are given in Figure 11. In all cases, the commercial polymer CR39 was used. The transparent hybrid polymers exhibit the characteristic coloring of the inserted dyes. We additionally show in Figure 11 (C) that ZL monolayer strongly scatters visible light (top). This phenomenon disappears completely when the monolayer is covered with a polymer film, giving rise to a perfectly transparent material (bottom).

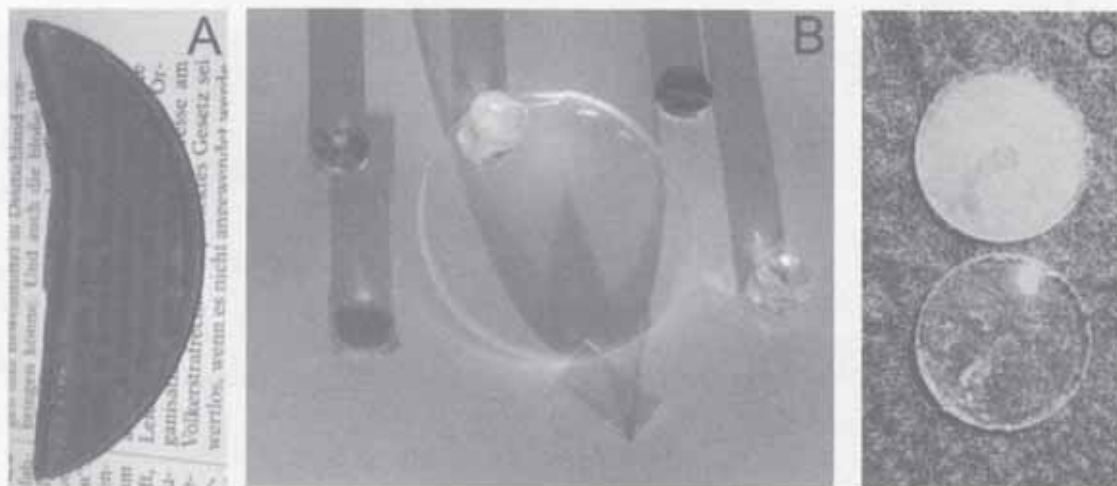


Figure 11 Photographic images of transparent polymer-ZL hybrid materials. (A): 1% w/w material prepared from Ox, HY3G, DMPOPOP-ZL in CR39. (B): selection of transparent dye-loaded and unloaded ZL-polymer hybrid materials. (C): unloaded ZL monolayers without (top) and with (bottom) CR39 coating

The hybrid polymer shown in Figure 11 (A) contains an energy transfer host-guest material based on the dyes Ox, HY3G and DMPOPOP; their structural formulae are given in Table 1. The UV-Vis absorption spectrum of this material is given in left part of Figure 12, while the luminescence spectra are shown on the right. The material exhibits three prominent absorption bands at 600 nm, at 482 nm, and at 395 nm corresponding to Ox, HY3G, and DMPOPOP, respectively. The curved baseline is due to Rayleigh scattering arising from the zeolites. This scattering is not strongly pronounced and the material is still very transparent in the visible range, as can be seen from the photographic image in Figure 11 (A).

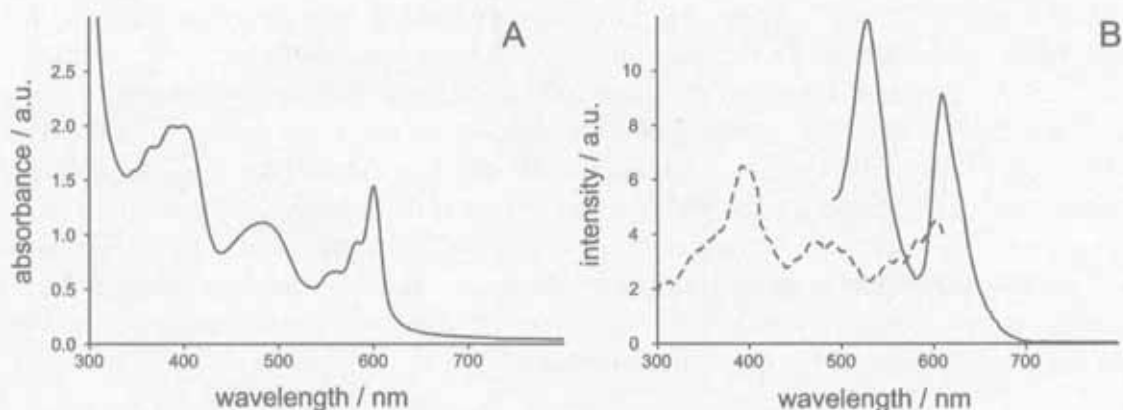
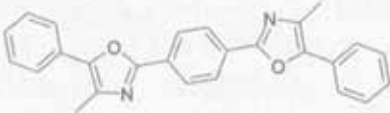
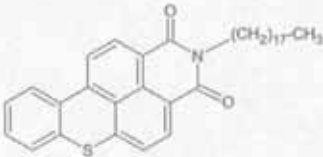
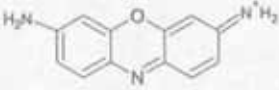


Figure 12 (A): Absorption spectrum of the hybrid material CR39-Ox, HY3G,DMPOPOP-ZL (1% w/w). (B): Excitation (dashed, $\lambda_{\text{det}} = 620$ nm) and emission (solid, $\lambda_{\text{ex}} = 420$ nm) spectra of the same material. The Ox emission at 605 nm is due to energy transfer from the donor dyes to the acceptor Ox

Table 1 Dyes used in the preparation of the hybrid material

		
DMPOPOP	HY3G	Ox

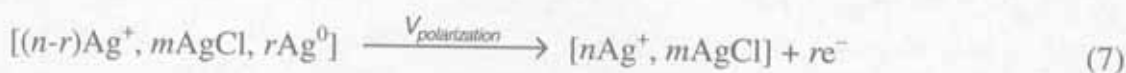
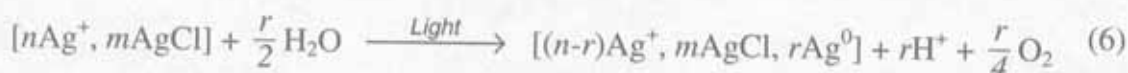
The functionality of the energy transfer system can be demonstrated by selectively exciting at 420 nm. The emission bands of both HY3G at 529 nm and Ox at 605 nm can be seen in this case. The excitation spectrum detected at 620 nm, where only Ox emits, exhibits excitation bands for all three dyes.

We conclude that new dye-ZL based building blocks are now ready to be tested in devices. Their size, morphology, and optical properties will need to be tailored to the specific task envisaged. The remaining problems to be solved require efforts at the interface of chemistry, physics, and engineering.

3 Photocatalytic and Photoelectrochemical Water Splitting

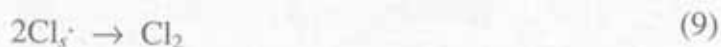
A large variety of photoactive materials have been studied in which zeolites host metal cations, clusters, or complexes as well as rare earth complexes.⁶⁴⁻⁷² Therefore, a complementary approach to what has been discussed in the previous chapter consists in integrating photochemically active substances into zeolite monolayers

coated on an electrode. This, in turn, allows taking advantage of intrazeolite processes for designing a reversible electrode for photocatalytic water oxidation. It has been shown that oxidation of water to O₂ can be photo catalysed by thin silver chloride layer deposited on a conducting support in the presence of an excess of silver ions.⁷³ The silver cations, which are adsorbed at the surface of silver chloride nanocrystals, are necessary for the reaction to proceed. Thus, light absorption can be considered to promote a charge-transfer from Cl⁻ to adsorbed Ag⁺. The light sensitivity in the visible spectral range is due to self-sensitization caused by reduced silver species. The overall stoichiometry of the reactions involved in the photooxidation of water to O₂ is the following:



To test their water splitting capability, Ag⁺/AgCl/Ag_n photo anodes were combined with an amorphous silicon solar cell. The AgCl layer was employed in the anodic part of a photoelectrochemical setup consisting of two compartments. A platinum electrode and an amorphous silicon solar cell were used in the cathodic part. Illumination of the Ag⁺/AgCl/Ag_n photoanode and the amorphous Si solar cell led to photoelectrochemical splitting of water to O₂ and H₂; see Figure 13 (left).⁷⁴ In other preliminary experiments, we prepared zeolite monolayers on conducting surfaces such as gold coated glass or gold foil.⁷⁵ These layers were prepared by either linking zeolite A (cubic) or ZL (disc-shaped) crystals to the gold surface through thioalcoxysilane molecules. The monolayers were further modified with Ag⁺ and AgCl. The so prepared AgCl/Ag⁺/Ag_n-zeolite photoanodes showed an increased water oxidation capability; see Figure 13 (right). We have good reasons to assume that oriented, dense ZL monolayers, consisting of disc shaped crystals – attached to the electrode with their bases and with a height of about 100 nm – will lead to a considerable improvement of these photoanodes for water oxidation.

According to eq. 6, water is oxidized to oxygen plus protons while silver cations are reduced to silver upon irradiation. Electrochemical reoxidation of the accumulated silver can be performed by anodic polarization of the electrode by means of a potentiostat, as shown in eq. 7. Both reactions take place simultaneously, making the system catalytic. The electron hole pairs formed upon illumination may recombine, or they may separate and produce silver atoms Ag⁰ and chlorine radicals Cl[•] (eq. 8). The Cl[•] radicals recombine very fast to form Cl₂ (eq. 9). The indices *s* and *i* in eqs. 8 and 9 refer to surface and interstitial species, respectively.



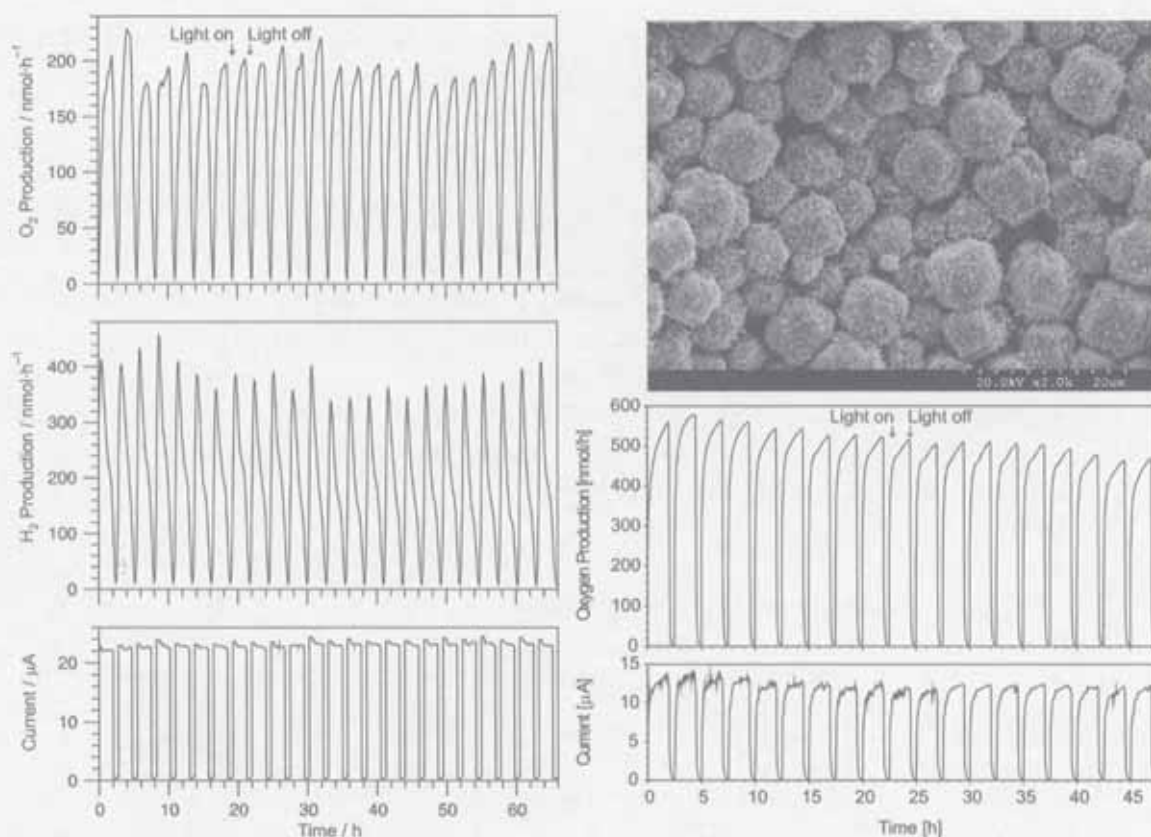
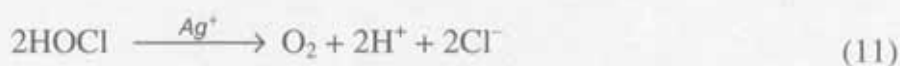


Figure 13 Photoelectrochemical experiments with $\text{AgCl}/\text{Ag}^+/\text{Ag}_n$ based photoanodes under illumination in the range of 350 nm to 700 nm in a flow system where the O_2 and H_2 were constantly removed (see refs. ⁷³⁻⁷⁵ for details). Left: O_2 and H_2 production and anodic photocurrent vs. time for an AgCl layer modified with Au colloids combined with a Pt cathode and an a-Si:H solar cell for several light and dark cycles.⁷⁴ Right: SEM image of an $\text{AgCl}/\text{Ag}^+/\text{Ag}_n$ modified zeolite A monolayer on a gold substrate (upper) and O_2 production and anodic photocurrent vs. time for an $\text{AgCl}/\text{Ag}^+/\text{Ag}_n$ -ZL electrode modified with Ag_2S in the ZL cavity⁷⁵

Under the applied conditions ($[\text{Ag}^+] \sim 10^{-3}$ M, pH \sim 4-6), Cl_2 reacts with water to form hypochloric acid; eq. 10. At lower pH and without excess Ag^+ in the electrolyte Cl_2 can be detected. Silver cations act as a catalyst for the decomposition of HOCl to molecular oxygen, protons and chloride ions; eq. 11. The chloride ions are bound by Ag^+ to form AgCl ; eq. 12. These reactions are very fast and it is reasonable to assume that they take place at or very close to the electrode surface.





Reduced silver atoms may react according to eq. 8, forming positively charged or neutral silver clusters. In its first stages, this reaction is related to the fundamental process of latent image formation in silver halides.⁷⁶



The self-sensitization of AgCl photoelectrochemical activity is due to silver clusters adsorbed on its surface. The silver cluster/silver chloride phase boundary is of particular importance for understanding all processes involved in the AgCl/Ag⁺/Ag_n electrode system. In the absence of an excess of Ag⁺ and silver clusters, pure AgCl does not absorb light below the indirect bandgap transition, which is in the near UV at about 3.3 eV.

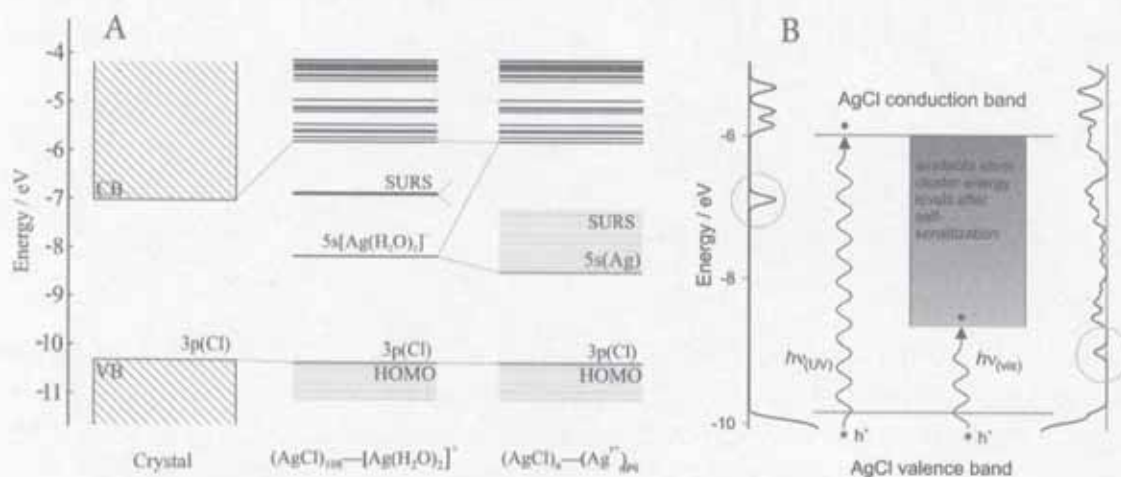


Figure 14 Electronic structure of an AgCl cluster modified with silver ions, hydrate silver ions and silvercluster on their surface. (A): Comparison of the electronic structure of an infinite AgCl crystal, a nano cluster with one [Ag(H₂O)₂]⁺ adsorbed on its surface and one with several of them adsorbed, some of them already reduced and therefore represented as (Ag_m^{r+})_{aq} with r smaller or equal to m. The crystal band gap and (AgCl)_n-(Ag_m^{r+})_{aq} values correspond to experimental values. SURS is the abbreviation for surface states.⁷⁷ (B): Proposed mechanism of self-sensitization. The density of levels (DOL) of a (AgCl)₁₉₂ cluster is shown on the left and the local density of levels (l-DOL) of the Ag₁₁₅-(AgCl)₁₉₂ composite is shown on the right. We observe new induced levels below the LUMO of the AgCl cluster. A schematical view is shown in the middle. The lowest lying levels into which electrons can be excited (marked with a circle) are metal induced gap states (MIGS). The position of the valence band is not markedly influenced by presence of the the Ag₁₁₅ cluster⁷⁸

A detailed discussion – from the perspective of solid state physics and photographic sensitivity – on the photoactivity of $\text{Ag}^+/\text{AgCl}/\text{Ag}_n$ has recently been reported by T. Tani.¹² Quantum chemical calculations and comparison of experimental with calculated values for the ionization energy of differently sized silver clusters shows that Ag levels are located below the conduction band edge of AgCl; Figure 14. Additional AgCl surface states (SURS), as well as metal induced gap states (MIGS) from Ag/AgCl cluster composites are present in the band gap region of silver chloride. These further levels are responsible for self-sensitization of silver chloride.^{77,78} They allow promotion of electrons to the conduction band, and hence creation of holes in the valence band, by light absorption below band gap energy. The energy of these transitions is lower than that needed for an optical transition from the AgCl valence band to its conduction band. Nevertheless, these new optical transitions in the visible spectral range can still initiate the oxidation of water since only the valence band is involved in that process. Thus, the photocatalytic oxidation of water on silver chloride is extended from the near UV into the visible range of the spectrum. This self-sensitization should not be confused with the spectral sensitization caused by silver clusters on silver chloride, also termed photographic Becquerel effect. The latter observation has been attributed to electron injection from electron-donating silver clusters into the AgCl conduction band. Addition of small amounts of gold clusters has been shown to improve the performance of the $\text{Ag}^+/\text{AgCl}/\text{Ag}_n$ photoanodes.⁷⁹ Very interesting observations have recently been reported on silver exchanged titanosilicates which might become of importance for this research field.⁸⁰ We also mention the existence of a plasmonic photocatalyst consisting of silver nanoparticles embedded in titanium dioxide.⁸¹ It is not yet understood to what extent the plasmon resonance states of the silver and gold clusters contribute to the behavior of the $\text{Ag}^+/\text{AgCl}/\text{Ag}_n$ system and further investigations would be of great interest.

One of the drawbacks of $\text{Ag}^+/\text{AgCl}/\text{Ag}_n$ photoanodes is the bad electron conductivity of silver chloride. Reversible systems could therefore be realized only with very thin layers, leading to insufficient light absorptivity. We have shown that the system can be improved by using zeolite monolayers as a support, which results in an increased surface area. The zeolites also act as a reservoir for the needed Ag^+ ions: regenerating them electrochemically (according to eq. 7) and keeping them close to the photoactive layer, so that they are not lost in the electrolyte. Preliminary results are encouraging despite the fact that the zeolite crystals used were too large and therefore the monolayer quality was insufficient. Great improvement can be expected by using an arrangement as shown in Figure 15, where the length of the crystals used to build the well oriented ZL monolayer is in the order of 100 nm or less. The layers must be prepared such that the channels are open in the direction of the photoactive surface and are well connected to the back electrode consisting of a thin gold layer e.g. coated on glass. Such experiments are now feasible due to the progresses achieved in ZL monolayer preparation.^{47,50-51,82}

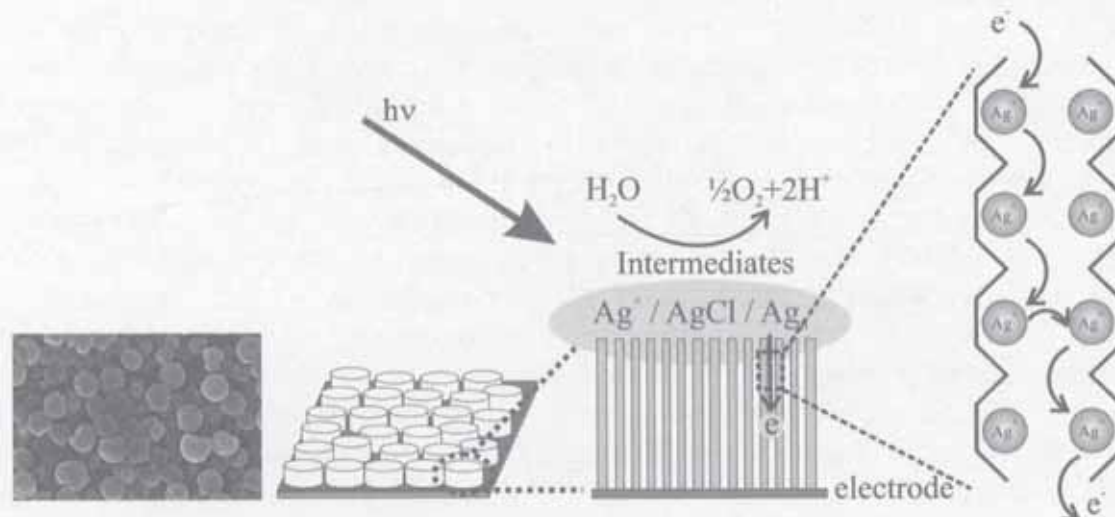


Figure 15 Scheme of an $\text{AgCl}/\text{Ag}^+/\text{Ag}_n\text{-ZL}$ based photoanode for photocatalytic water oxidation. Left: Monolayer consisting of less than 100 nm thick oriented ZL crystals with a diameter of about 600 nm. Middle: schematic view of a modified ZL monolayer. Right: scheme of a single ZL crystal fixed on a gold electrode and modified with $\text{Ag}^+/\text{AgCl}/\text{Ag}_n$. The zeolite is fully exchanged with silver ions and may also contain some reduced silver particles. The processes taking place in the box "intermediates" are explained in eqs. 6-12. Electron conductivity and photoactivity can be enhanced by adding small gold clusters

4 Conclusions

Zeolites and mesoporous silica are versatile host materials for the supramolecular organization of a large variety of guests. The inclusion of photoactive molecules, complexes, or clusters into ordered one-dimensional channel systems is particularly intriguing, as the resulting host-guest compounds may exhibit properties such as optical anisotropy, efficient energy transfer, enhanced stability or specific photo activity. Several levels of organization have been realized for ZL, extending from the interior of a given crystal to the channel entrances and the external surface as well as from the microscopic to the macroscopic scale. A broad array of chemistries has been involved in the development of highly organized and functional host-guest objects. Of particular interest is the design of molecules which are able to selectively adsorb at the channel entrances. Such molecules can establish communication between included guests and external objects. These highly organized host-guest materials offer great opportunities for the design of novel building blocks for photovoltaic applications, luminescent solar concentrators or for photocatalytical water splitting, but also for being used in other kind of photoelectronic or sensing devices. The new guest-ZL based building blocks are currently being tested in devices. Their size, morphology, composition and optical properties need to be tailored to the specific task envisaged. The problems to be solved for realizing practical devices require efforts at the interface of chemistry, physics, and

engineering. Zeolite based materials are more advanced with respect to the organizational level and to the realization of practical applications, than materials based on mesoporous hosts.^{7,9} The latter are, however, catching up.⁸³⁻⁸⁴ It has been discussed that, despite the obvious differences between microporous and mesoporous host-guest materials, many similarities and analogies exist.⁹ Therefore potentially allowing for the transfer of concepts presented here to mesoporous based materials.

Acknowledgements

We would like to thank Roman Calzaferri for realizing Figure 1. A. D. acknowledges the European Commission through the Human Potential Program (Marie-Curie RTN Nanomatch, Grant N0. MRTN.CT-2006-035884).

5 References

- [1] N. Armaroli, V. Balzani, *Angew. Chem. Int. Ed.* **2007**, *46*, 52-66.
- [2] C. B. Field, M. J. Behrenfeld, J. T. Randerson, P. Falkowski, *Science*, **1998**, *281*, 237-240.
- [3] G. R. Davis, *Scientific American* **1990**, *263*, 21-27.
- [4] W. Ostwald, *Die Mühle des Lebens*, Theod. Thomas Verlag, Leipzig, **1911**
- [5] G. Ciamician, *Science* **1912**, *36*, 385-394.
- [6] a) V. Balzani, A. Credi, M. Venturi, *ChemSusChem* **2008**, *1*, 26-58; b) A. C. Benniston, A. Harriman, *Mater Today* **2008**, *11*, 26-34.
- [7] a) G. Calzaferri, K. Lutkouskaya, *Photochem. Photobiol. Sci.* **2008**, *7*, 879-910; b) G. Calzaferri, S. Huber, H. Maas, C. Minkowski, *Angew. Chem. Int. Ed.* **2003**, *42*, 3732-3758.
- [8] E. Johansson, E. Choi, S. Angelos, M. Liong, J. I. Zink, *J. Sol-Gel Sci. Technol.* **2008**, *46*, 313-322.
- [9] D. Brühwiler, G. Calzaferri, T. Torres, J.H. Ramm, N. Gartmann, L.-Q. Dieu, I. López-Duarte, M. Martínez Díaz, *J. Mater. Chem.* **2009**, *19*, 8040-8067.
- [10] a) S. Hashimoto, K. Samata, T. Shoji, N. Taira, T. Tomita, S. Matsuo, *Micropor. Mesopor. Mater.* **2009**, *117*, 220-227; b) J. S. Lee, K. Ha, Y. J. Lee, K. B. Yoon, *Top. Catal.* **2009**, *52*, 119-139.
- [11] a) A. J. Bard, M. A. Fox, *Acc. Chem. Res.* **1995**, *28*, 141-145; b) D. Gust, T. A. Moore, A. L. Moore, *Acc. Chem. Res.* **2001**, *34*, 40-48.
- [12] T. Tani, *J. Soc. Photogr. Sci. Technol. Japan* **2009**, *72*, 88-94.
- [13] F. E. Osterloh, *Chem. Mater.* **2008**, *20*, 35-54.
- [14] A. Currao, *Chimia* **2007**, *61*, 815-819.
- [15] T. Pullerits, V. Sundström, *Acc. Chem. Res.* **1996**, *29*, 381-389.
- [16] Th. Förster, *Ann. Physik (Leipzig)* **1948**, (6) *2*, 55-75.
- [17] G. Calzaferri, N. Gfeller, *J. Phys. Chem.* **1992**, *96*, 3428-3435.

- [18] G. Calzaferri, M. Pauchard, H. Maas, S. Huber, A. Khatyr, T. Schaafsma, *J. Mater. Chem.* **2002**, *12*, 1-13.
- [19] V. Ramamurthy, *Photochemistry in Organized and Constrained Media*. VCH publishers, NY, **1991**.
- [20] N. J. Turro, *Acc. Chem. Res.* **2000**, *33*, 637-646.
- [21] S. Hashimoto, *J. Photochem. Photobiol. C: Photochem. Rev.* **2003**, *4*, 19-49.
- [22] A. M. Abeykoon, M. Castro-Colin, E. V. Anokhina, M. N. Iliev, W. Donner, A. J. Jacobson, S. C. Moss, *Phys. Rev. B* **2008**, *77*, 075333 (1-10).
- [23] S. Hashimoto, M. Yamaji, *Phys. Chem. Chem. Phys.* **2008**, *10*, 3124-3130.
- [24] J. Zhu, Y. Huang, *J. Phys. Chem. C* **2008**, *112*, 14241-14246.
- [25] G. Schulz-Ekloff, D. Wöhrle, B. van Duffel, R. A. Schoonheydt, *Micropor. Mesopor. Mater.* **2002**, *51*, 91-138.
- [26] A. Corma, H. Garcia, *Eur. J. Inorg. Chem.* **2004**, 1143-1146.
- [27] M. Tsotsalas, M. Busby, E. Gianolio, S. Aime, L. De Cola, *Chem. Mater.* **2008**, *20*, 5888-5893.
- [28] H. S. Kim, T. T. Pham, K. B. Yoon, *J. Am. Chem. Soc.* **2008**, *130*, 2134-2135.
- [29] B. Bussemer, I. Dreiling, U. W. Grummt, G. J. Mohr, *J. Photochem. Photobiol. A: Chemistry* **2009**, *204*, 90-96.
- [30] S. Megelski, G. Calzaferri, *Adv. Funct. Mater.* **2001**, *11*, 277-286.
- [31] A. Zabala Ruiz, D. Brühwiler, T. Ban, G. Calzaferri, *Monatshefte f. Chemie* **2005**, *136*, 77-89.
- [32] A. Zabala Ruiz, D. Brühwiler, L.-Q. Dieu, G. Calzaferri, in: U. Schubert, N. Hüsing, R. Laine (eds) *Materials Syntheses A Practical Guide*, Springer Wien (ISBN 978-3-211-75124-4) **2008**, pp 9-19
- [33] T. Ohsuna, B. Slater, F. Gao, J. Yu, Y. Sakamoto, G. Zhu, O. Terasaki, D. E. Vaughan, S. Qiu, C. R. Catlow, *Chem. Eur. J.* **2004**, *10*, 5031- 5040.
- [34] O. Larlus, V. P. Valtchev, *Chem. Mater.* **2004**, *16*, 3381- 3389.
- [35] Y. J. Lee, J.S. Lee, K. B. Yoon, *Micropor. Mesopor. Mater.* **2005**, *80*, 237-246.
- [36] Y. Lee, C. C. Kao, S. J. Kim, H. H. Lee, D. R. Lee, T. J. Shin, J. Y. Choi, *Chem. Mater.* **2007**, *19*, 6252-6257.
- [37] R. Brent, M. W. Anderson, *Angew. Chem. Int. Ed.* **2008**, *47*, 5327-5330.
- [38] D. W. Breck, *Zeolite Molecular Sieves*, John Wiley & Sons, NY, **1974**.
- [39] a) Ch. Baerlocher, W. M. Meier, D. H. Olson, *Atlas of Zeolite Framework Types*, Elsevier, Amsterdam, **2001**, 5th edn; b) International Zeolite Association, <http://www.iza-structure.org>
- [40] M. Pauchard, A. Devaux, G. Calzaferri, *Chem. Eur. J.* **2000**, *6*, 3456-3470.
- [41] G. Calzaferri, *Il Nuovo Cimento* **2008**, *123 B*, 1337-1367.
- [42] G. Calzaferri, A. Devaux, in: V. Ramamurthy, Y. Inoue (eds) *Supramolecular Effects in Photochemical Photophysical Processes*, John Wiley & Sons, in press.
- [43] A. S. Davydov, *Usp. Fiz. Nauk* **1964**, *82*, 145-178.

- [44] M. Busby, C. Blum, M. Tibben, S. Fibikar, G. Calzaferri, V. Subramaniam, L. De Cola, *J. Am. Chem. Soc.* **2008**, *130*, 10970-10976.
- [45] G. Calzaferri, patents EP1335879, US6932919, US7372012.
- [46] H. Maas, G. Calzaferri, *Angew. Chem. Int. Ed.* **2002**, *41*, 2284-2288.
- [47] K. B. Yoon, *Acc. Chem. Res.* **2007**, *40*, 29-40.
- [48] S. Huber, G. Calzaferri, *Angew. Chem. Int. Ed.* **2004**, *43*, 6738-6742.
- [49] M. Busby, H. Kerschbaumer, G. Calzaferri, L. De Cola, *Adv. Mater.* **2008**, *20*, 1614-1618.
- [50] a) A. Zabala Ruiz, H. Li, G. Calzaferri, *Angew. Chem. Int. Ed.* **2006**, *45*, 5282-5287; b) G. Calzaferri, A. Zabala Ruiz, H. Li, S. Huber, patent WO 2007/012216.
- [51] F. Cucinotta, Z. Popovic', E. A. Weiss, G. M. Whitesides, L. De Cola, *Adv. Mater.* **2009**, *21*, 1142-1145.
- [52] a) V. Vohra, D. Devaux, L.-Q. Dieu, G. Scavia, M. Catellani, G. Calzaferri, C. Botta, *Adv. Mater.* **2009**, *21*, 1146-1150; b) V. Vohra, A. Bolognesi, G. Calzaferri, C. Botta, *Langmuir*, **2009**, *25*, 12019-12023.
- [53] a) S. Suárez, A. Devaux, J. Bañuelos, O. Bossart, A. Kunzmann, G. Calzaferri, *Adv. Func. Mater.* **2007**, *17*, 2298-2306; b) H.J. Metz, G. Calzaferri, S. Suarez, A. Devaux, A. Kunzmann, patent EP 1873202B1, US 7655300B2.
- [54] R. Koeppe, O. Bossart, G. Calzaferri, N. S. Sariciftci, *Sol. Ener. Mat. Sol. Cells.* **2007**, *91*, 986-995.
- [55] R. L. Garwin, *Rev. Sci. Instr.* **1960**, *31*, 1010-1011.
- [56] W. H. Weber, J. Lambe, *Appl. Opt.* **1976**, *15*, 2299-2300.
- [57] A. Goetzberger, W. Greubel, *Appl. Phys.* **1977**, *14*, 123-139.
- [58] J. S. Batchelder, A. H. Zewail, T. Cole, *Appl. Opt.* **1979**, *18*, 3090-3110.
- [59] a) P. Kittidachachan, L. Danos, T. J. Meyer, N. Alderman, T. Markvart, *Chimia* **2007**, *61*, 780-786; b) D. Brühwiler, L.-Q. Dieu, G. Calzaferri, *Chimia* **2007**, *61*, 820-822.
- [60] M. J. Currie, J. K. Mapel, T. D. Heidel, S. Goffri, M. A. Baldo, *Science* **2008**, *321*, 226-228.
- [61] a) G. Calzaferri, H. Li, D. Brühwiler, *Chem. Eur. J.* **2008**, *14*, 7442-7449; b) G. Calzaferri, A. Kunzmann, D. Brühwiler, Ch. Baur, Patent CH-698333.
- [62] a) N. Tessler, V. Medvedev, M. Kazes, S. Kan, U. Banin, *Science*, **2002**, *295*, 1506-1508; b) O. Kalinina, E. Kumacheva, *Chem. Mater.* **2001**, *13*, 35-38; c) I. Gourevich, H. Pham, J. E. N. Jonkman, E. Kumacheva, *Chem. Mater.* **2004**, *16*, 1472-1479; d) M. Avella, M. E. Errico, E. Martuscelli, *Nano Lett.* **2001**, *1*, 213-217.
- [63] J. Schneider, D. Fanter, M. Bauer, C. Schomburg, D. Wöhrle, G. Schulz-Ekloff, *Micropor. Mesopor. Mater.* **2000**, *39*, 257-263.
- [64] J. K. Thomas, *Chem. Rev.* **2005**, *105*, 1683-1734.
- [65] F. Laeri, F. Schueth, U. Simon, M. Wark (eds), *Host-Guest Systems Based on Nanoporous Crystals*, VCH, Weinheim, Germany, **2003**.

- [66] G. Calzaferri, C. Leiggenger, S. Glaus, D. Schürch, K. Kuge, *Chem. Soc. Rev.* **2003**, *32*, 29-37.
- [67] G. De Cremer, Y. Antoku, M. B. Roeffaers, M. Sliwa, J. Van Noyen, S. Smout, J. Hofkens, D. E. De Vos, B. F. Sels, T. Vosch, *Angew. Chem. Int. Ed.* **2008**, *47*, 2813-2816.
- [68] G. De Cremer, E. Coutiño-Gonzalez, M. B. Roeffaers, B. Moens, J. Ollevier, M. Van der Auweraer, R. Schoonheydt, P. A. Jacobs, F. C. De Schryver, J. Hofkens, D. E. De Vos, B. F. Sels, T. Vosch, *J. Am. Chem. Soc.* **2009**, *131*, 3049-3056.
- [69] S. H. Kim, T. N. Thi, N. H. Heo, G. H. Kim, S. B. Hong, J. D. Head, K. Seff, *J. Phys. Chem. C* **2008**, *112*, 11181-11193.
- [70] D. Sendor, U. Kynast, *Adv. Mater.* **2002**, *14*, 1570-1574.
- [71] M. Lezhnina, F. Laeri, L. Benmouhadi, U. Kynast, *Adv. Mater.* **2006**, *18*, 280-283.
- [72] Y. Wang, H. Li, L. Gu, Q. Gan, Y. Li, G. Calzaferri, *Micropor. Mesopor. Mater.* **2009**, *121*, 1-6.
- [73] D. Schürch, A. Currao, S. Sarkar, G. Hodes, G. Calzaferri, *J. Phys. Chem. B* **2002**, *109*, 12764-12775.
- [74] A. Currao, V. R. Reddy, M. K. van Veen, R. E. Schropp, G. Calzaferri, *Photochem. Photobiol. Sci.* **2004**, *3*, 1017-1025.
- [75] a) V. R. Reddy, A. Currao, G. Calzaferri, *J. Mater. Chem.* **2007**, *17*, 3603-3609; V. R. Reddy, PhD thesis, Modified AgCl Photoanodes for Water Oxidation and Water Splitting, University of Bern **2006**; c) C. Leiggenger, G. Calzaferri, *ChemPhysChem* **2004**, *5*, 1593-1596.
- [76] T. Tani, *Photographic Sensitivity*, Oxford University Press, NY, **1995**.
- [77] S. Glaus, G. Calzaferri, *J. Phys. Chem. B* **1999**, *103*, 5622-5630.
- [78] S. Glaus, G. Calzaferri, R. Hoffmann, *Chem. Eur. J.* **2002**, *8*, 1786-1794.
- [79] A. Currao, V.R. Reddy, G. Calzaferri, *ChemPhysChem* **2004**, *5*, 720-724.
- [80] G. Agostini, S. Usseglio, E. Groppo, M.J. Uddin, C. Prestipino, S. Bordiga, A. Zecchina, P.L. Solari, C. Lamberti, *Chem. Mater.* **2009**, *21*, 1343-1353.
- [81] K. Awazu, M. Fujimaki, C. Rockstuhl, J. Tominaga, H. Murakami, Y. Ohki, N. Yoshida, T. Watanabe, *J. Am. Chem. Soc.* **2008**, *130*, 1676-1680.
- [82] a) Y. Wang, H. Li, B. Liu, Q. Gan, Q. Dong, G. Calzaferri, Z. Sun, *J. Solid. State. Chem.* **2008**, *181*, 2469-2472; b) H. Li, Y. Wang, W. Zhang, B. Liu, G. Calzaferri, *Chem. Commun.* **2007**, 2853-2854; c) Y. Wang, H. Li, Y. Feng, H. Zhang, G. Calzaferri, T. Ren, *Angew. Chem. Int. Ed.* **2010**, *49*, 1434-1438.
- [83] a) S. Inagaki, O. Othani, Y. Goto, K. Okamoto, M. Ikai, K. Yamanaka, T. Tani, T. Okada, *Angew. Chem. Int. Ed.* **2009**, *48*, 4042-4046; b) N. Gartmann, D. Brühwiler, *Angew. Chem. Int. Ed.* **2009**, *48*, 6354-6356.
- [84] V. Valtchev, S. Mintova, M. Tsapatsis, *Ordered Porous Solids, Recent Advances and Prospects*, Elsevier ISBN 978-0-444-53189-6, **2009**.